Heliyon 5 (2019) e02651

Contents lists available at ScienceDirect

Heliyon

journal homepage: www.heliyon.com

Research article

The numerical simulation and experimental study of heat release in a heat storage system with various diameters of aluminum tubes

Zhengbin He *, Qian Wan, Zhenyu Wang, Jiali Zhang, Songlin Yi **

Beijing Key Laboratory of Wood Science and Engineering, College of Material Science and Technology, Beijing Forestry University, Beijing, 100083, PR China

ARTICLE INFO

Keywords:
Energy
Energy storage technology
Solar energy
Energy sustainability
Energy conservation
Energy use in building
Urban energy consumption
Phase change material (PCM)
Heat release
Simulation
Aluminum tube diameter

ABSTRACT

Phase change materials (PCMs) can be used to store solar energy. The heat released from PCMs is directly influenced by the efficiency of thermal energy storage and the scope of application. In this study, paraffin was used as the PCM, and was encapsulated in an aluminum tube. The temperature of the inner PCM was measured, and the heat release process of the PCM was simulated. The results indicate that the melt temperature of the PCM ranged from 45 °C to 60 °C, and the latent heat was 177 J/g. The heat release processes of the PCM in different aluminum tubes included three stages: 1) the stage during which no phase change occurred at temperatures above the melt temperature and at a rapidly decreasing temperature; 2) the stage during which phase change occurred at very slowly decreasing temperatures; 3) the stage during which no phase change occurred at temperatures lower than the melt temperature. The temperature of the PCM decreased when the radius of the aluminum tube increased. The temperature results obtained via simulation were similar to the actual temperature data. The total energy released from the PCM increased linearly with the time required to complete the energy release process of the PCM in aluminum tubes with different diameters, as well as with the increase in the aluminum tube diameter. The diameter of the PCM exerted no significant influence on the energy release rate. The relationship between the tube diameter and the time required to complete heat release, and the relationship between the amount of heat released, the diameter of the aluminum tube, and the release time, were established. These equations could predict actual values and provide theoretical guidance for heat release in heat storage systems. They could also be used as a guide in practical production.

1. Introduction

The increased consumption of fossil fuels and excessive CO_2 emissions in recent years has resulted in major environmental issues worldwide [1]. Food and wood drying can effectively address the spoilage of foods such as fruits, vegetables, and grains. The technique can also reduce defects of wood products including timber architecture, furniture, and floors in building and construction. The drying process consumes a large amount of energy; and it uses about 10%–15% of the overall global industrial energy [2, 3].

Solar radiation energy that exceeds the global energy demand by more than 10,000 times could be received by Earth every year [4, 5]. Solar drying also has a relatively low cost energy, and the construction of a solar dryer is a relatively simple process [4, 6]. Moreover, after solar drying, foods, medicinal herbs, and plant perfume materials could retain their flavor, texture, taste and nutrients, or color. In addition, wood solar drying method in particular involves considerably fewer drying defects, such as deformations and cracks [7, 8, 9]. Solar drying can extend the storage and spoilage of stored materials [10, 11, 12]. The solar dryer is one of the most high-potential applications of solar energy due to its ability to produce solar energy and contribute a significant amount of heat to food, wood products, and other biomass needed for drying, as well as its ability extract moisture from the dried material without affecting its quality [12, 13, 14]. Solar energy, a type of renewable energy, can thus reduce the consumption of conventional sources of energy, such as fossil fuels. The use of solar energy is the optimal method for reducing the cost of energy and decreasing CO_2 emissions during food, vegetable, and wood drying [15, 16, 17].

* Corresponding author.
** Corresponding author.
E-mail addresses: hzbcailiao@bjfu.edu.cn (Z. He), ysonglin@bjfu.edu.cn (S. Yi).

https://doi.org/10.1016/j.heliyon.2019.e02651
Received 29 July 2019; Received in revised form 23 September 2019; Accepted 9 October 2019

Solar energy drying provides numerous advantages; however, its intermittent generation prevents its application at nighttime and during rainy and cloudy conditions. The absence of solar energy during drying could cause material spoilage and other defects [18]. Heat storage systems with PCMs can address such problems [19, 20]. Many studies have been conducted to develop solar drying kilns with a storage system [21, 22, 23]. We built a large number of commercial solar drying kilns with a heat storage system that absorbs heat during the daytime when redundant solar energy exists, and releases heat during night to dry material; the solar energy could be stored during the daytime and reused during the night. These systems were used in many factories, and test results indicated that the temperature of the inner kiln could reach 64.8 °C [24], which is an ideal condition for food and wood drying.

The proposed solar drying kiln can be used to a certain degree in the drying processes of food, wood, and other biomass. No studies have been conducted on the heat release process in heat storage systems. Heat release is one of the most important parameters for heat storage systems, and directly influences heat efficiency, drying efficiency, and drying time. To understand the heat release process of a heat storage system with a PCM, and to guide the preparation of a drying schedule with low energy costs and high drying efficiency, paraffin encapsulated in an aluminum tube was used as the PCM to construct the heat storage system. The temperature distribution, heat release process, and effects of the aluminum tube diameter on the heat release process were evaluated.

2. Materials and method

2.1. Materials and equipment

(1) Materials

The solar drying temperature usually varies from 45 °C to 80 °C [15, 25]. Thus, paraffin, which has a melt point in this temperature range, was used as the PCM in the heat storage system. Paraffin is chemically inert, noncorrosive, odorless, durable, inexpensive, easily available, ecologically harmless, and nontoxic [26]. In addition, paraffin exhibits little or no super cooling property, low vapor pressure, good thermal and chemical stability, and a self-nucleating behavior [27]. To prevent paraffin pollution and to apply it conveniently, the paraffin was encapsulated in an aluminum tube to establish the energy storage system.

(2) Equipment

The drying kiln was used to simulate the solar drying process. The schematic of a drying kiln with a heat storage system and a temperature collecting system is presented in Fig. 1.

2.2. Method

2.2.1. Characteristics of the PCM

Differential scanning calorimetry (DSC) was conducted to measure the heat characteristics of the PCM, including the phase change temperature and latent heat.

2.2.2. Heat release process of the PCM

Both heat storage and heat release can influence the energy storage efficiency of the PCM. In practice, heat storage is always coupled with material drying when surplus energy is available during the day-time [24]; additionally, heat release always begins at night when solar energy is insufficient. Thus, heat release is a key parameter that contributes to the efficiency of the heat storage system. The temperature inside the solar drying kiln during use can reach 65 °C–70 °C based on the study of some commercial driers. Thus, to simulate the practical solar drying process, the initial temperature of the PCM was set to 70 °C in this study.

During the experiment, temperature sensors were installed in the PCM, and the PCM in the aluminum tube was heated in a water bath (JianLejie Limited Company, Beijing) at a constant temperature of 70 °C. The aluminum tube was then installed in a custom-designed drying oven (Fig. 1), which was a small-scale version of the drying kiln. The velocity of the medium (air) in the drying oven was 1.0 m/s, and was controlled using a fan and a velocity transducer. The fan changed its direction every 10 min. The temperature of the medium in the kiln was 25 °C, and was controlled by ventilation. The temperature at different times was collected using a temperature collecting and recording system. Comsol Software (Comsol Inc., USA), which is a general-purpose simulation software for modeling designs, devices, and processes in all fields of engineering, manufacturing, and scientific research, was used to simulate heat release.

3. Model

The PCM cooling process is heat transfer coupled with phase change. During heat release, the fan changes its rotation direction at intervals of 5 min to ensure that the heat synchronously exchanges around the tube wall, heat transfers from the aluminum tube wall to the medium in the drying kiln by convection, and heat transfers to the aluminum wall from the PCM by conduction (as shown in Fig. 2).

3.1. Assumptions

The assumptions for the heat release process of the PCM are as follows:

1) The PCM is symmetric along the axis.
2) No PCM moves in the length and radial directions.

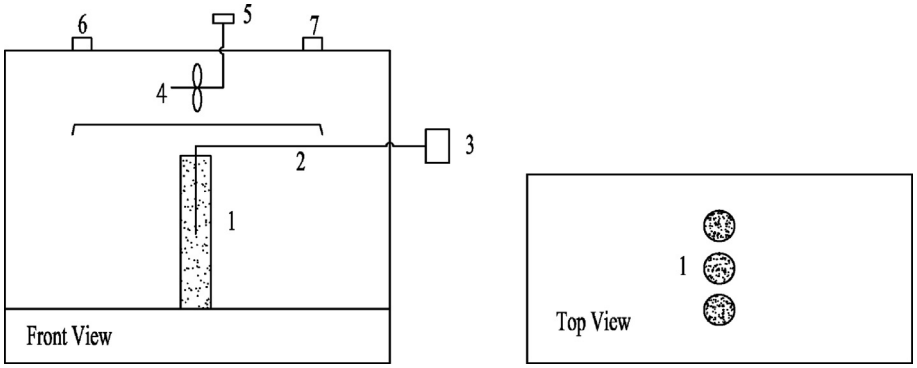

Fig. 1. Schematic of the aluminum tube arrangement in the drying kiln. 1) aluminum tube with PCM; 2) temperature sensor and connection line; 3) temperature collecting and recording system; 4) fan to act as the velocity of the drying medium; 5) velocity transducer to change the velocity of the drying medium; 6) and 7) left and right ventilation to allow the exchange of air from the environment.

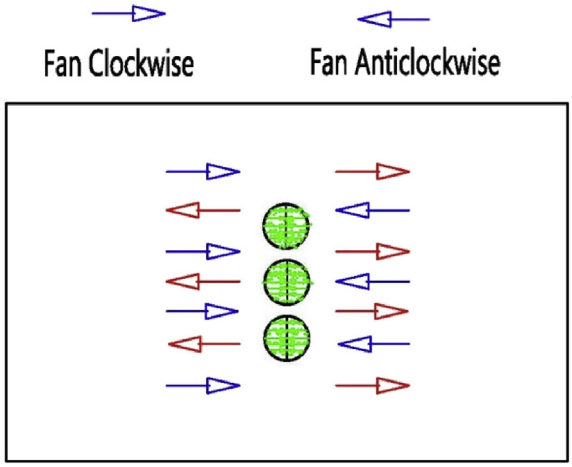

Fig. 2. Heat transfer during PCM heat release.

3) No chemical reaction occurs during this stage, and no heat is generated inside the heat storage system.
4) To simplify the process, one aluminum tube in the heat storage system was studied.
5) No heat transition occurs at the top and bottom of the PCM because of a 10 mm thermal insulation material at the top and bottom of the aluminum tube.

3.2. Geometry of the samples

The geometry of the PCM in the aluminum tube is presented in Fig. 3. The height of the aluminum tube measured 280 mm, including the 10 mm thermal insulation material at the top and bottom of the aluminum tube. The thickness of the aluminum tube was 1 mm. Based on these assumptions, the heat transfer for PCM heat release can be simplified as a 2D model of its cross-section (ABCD). The DC boundary is the symmetry boundary in the radial direction with no heat transfer, and convective heat transfer occurs at the AB boundary.

3.3. Heat transfer model

Based on these assumptions, the general heat transfer equations, boundary conditions, and initial conditions for the cross-section (ABCD) were as follows:

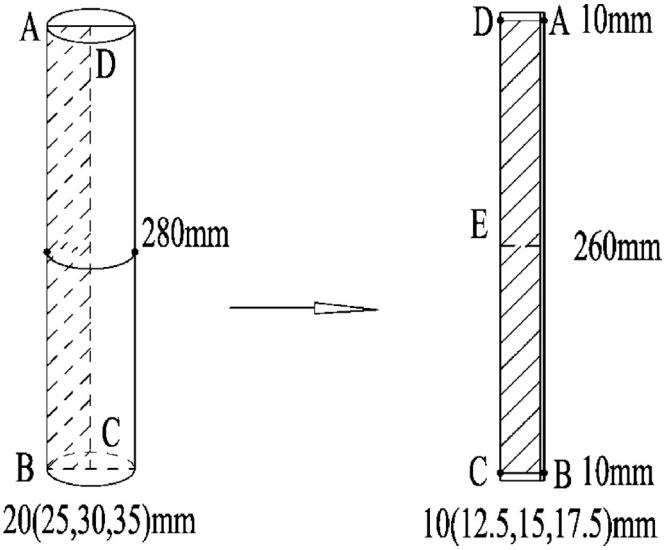

Fig. 3. Geometry and cross section (ABCD) of the PCM in the aluminum tube.

(1) General heat transfer equation:

Heat transfer,

$$\frac{\partial t}{\partial \tau} = \frac{\lambda}{\rho c}\frac{\partial^2 t}{\partial x^2} + \frac{Q}{\rho c} \tag{1}$$

(2) Boundary conditions:

Heat transfer,

$$\mathbf{n}\cdot(-\lambda\nabla T) = 0 \quad \text{At boundary AD, BC and DC} \tag{2}$$

$$\mathbf{n}\cdot(\lambda\nabla T) + Q = h(T_p - T_w) \quad \text{At boundary AB} \tag{3}$$

(3) Initial conditions:

$$t(x,y)|_{\tau=0} = t_0 \tag{4}$$

where, t is the temperature of PCM, °C; τ is time, min; λ is the thermal conductivity of the PCM, W/(m·K); ρ is the density of the PCM, kg/m^3; c is the specific heat of the PMC, kJ/(kg·K); Q is the latent heat, kJ; h is the heat transfer coefficient, W/(m^2·K); T_p is the temperature at boundary AB, °C; T_w is the temperature in the drying medium, °C; and t_0 is the initial temperature of the PCM, °C.

The parameters are listed in Table 1 [27,28].

4. Results and discussion

4.1. Characteristics of the PCM

DSC can be used to measure the specific heat, latent heat, and melting range of the PCM. The melting range is commonly known as the "mushy zone" within which the PCM first softens and then melts [29]. The melting range is shown in Fig. 4. The first peak occurs at around 38 °C; it presents the solid-to-solid phase transition, and is attributed to a disordering of the monoclinic crystal to a pseudohexagonal crystal [28]. The second peak is at around 56 °C, which is the melting transition. The mushy zone for the PCM is not a point but a zone; the melt transition ranges from 45 °C to 60 °C, and the latent heat is 177 J/g. The specific heat range is from 1.24 to 31.71 J/(g· °C) during the phase change.

4.2. Temperature distribution in PCM tubes with different diameters

The PCM was entirely liquid during the first stage of the heat release process. Some PCM around the tube became solid when the medium in the drying kiln flowed through the aluminum tube and removed energy from the PCM. Meanwhile, the PCM was entirely liquid at the center of the tube, and both liquid and solid PCM are observed between the solid and liquid PCM during the second stage. During the third stage, most of the energy was removed by the medium in the drying oven, and the PCM became entirely solid. A schematic of the phase variations is presented in

Table 1
Parameters of the PCM and the aluminum tube.

Parameters	Value	Parameters	Value
t_0	70	λ_l	0.167–0.437
T_w	26	h	10–13.5
ρ_s	900	ρ_a	2680
ρ_l	700	λ_a	227
λ_s	0.2964–0.466	c_a	0.947

Subscript *s*, *l*, and *a* are represent solid paraffin, liquid paraffin, and the aluminum tube, respectively.

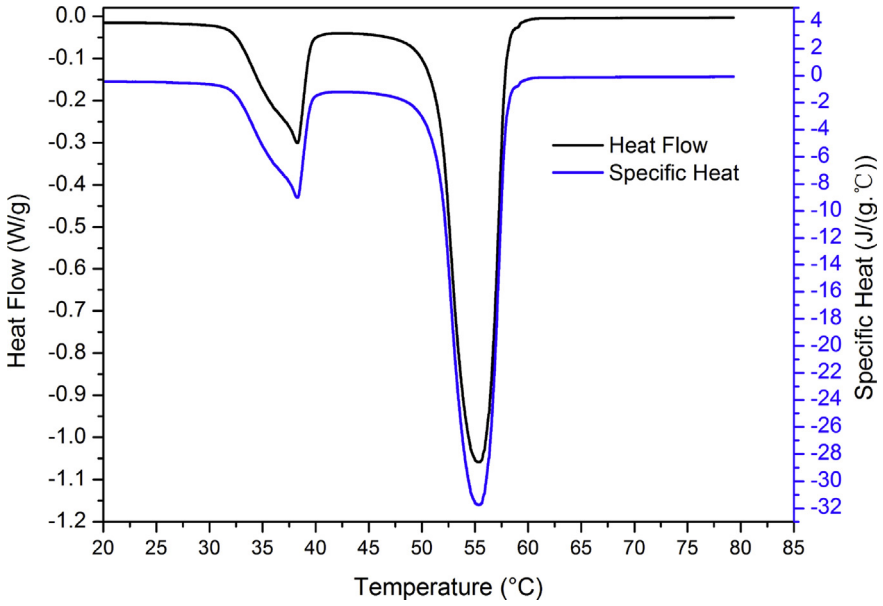

Fig. 4. Thermal characteristics of the PCM.

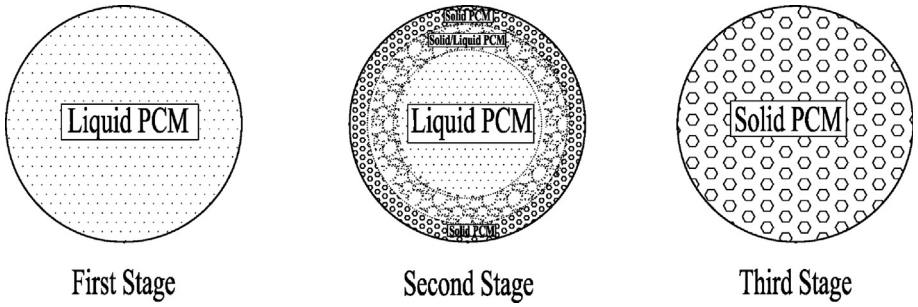

Fig. 5. Phase variations of the PCM at different times.

Fig. 5. Both latent heat and sensible heat were released during the phase change and temperature variation.

The temperature distribution of the PCM at the three stages in aluminum tubes with different diameters is discussed, including the heat variations of the PCM in the following scenarios: 1) no phase change; 2) partial phase change; 3) total phase change to solid.

Figs. 6, 7, 8, and 9 respectively present the temperature distributions of PCM in aluminum tubes with diameters of 20, 25, 30, and 35 mm during heat release. To better understand the temperature of PCM variation, the temperatures of the PCM in the tubes with different diameters

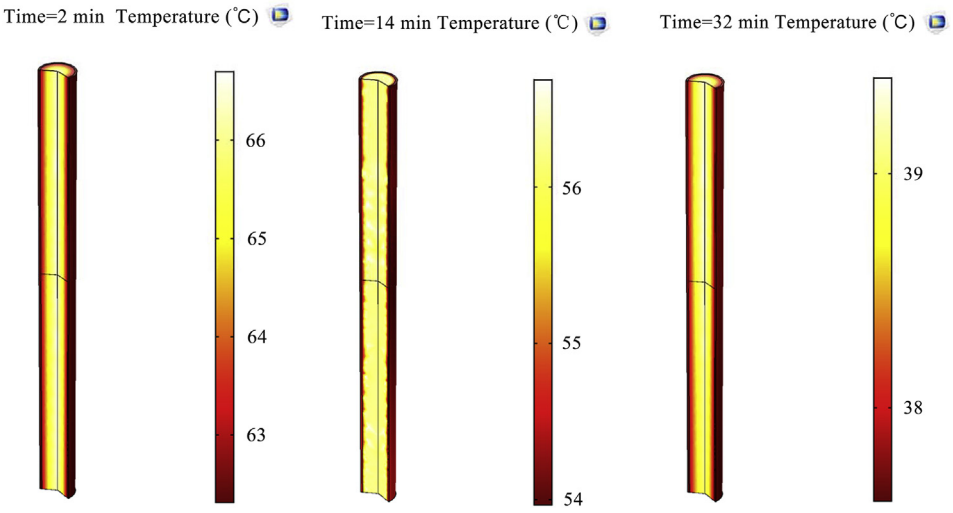

Fig. 6. Temperature distribution of the PCM in the tube with a diameter of 20 mm.

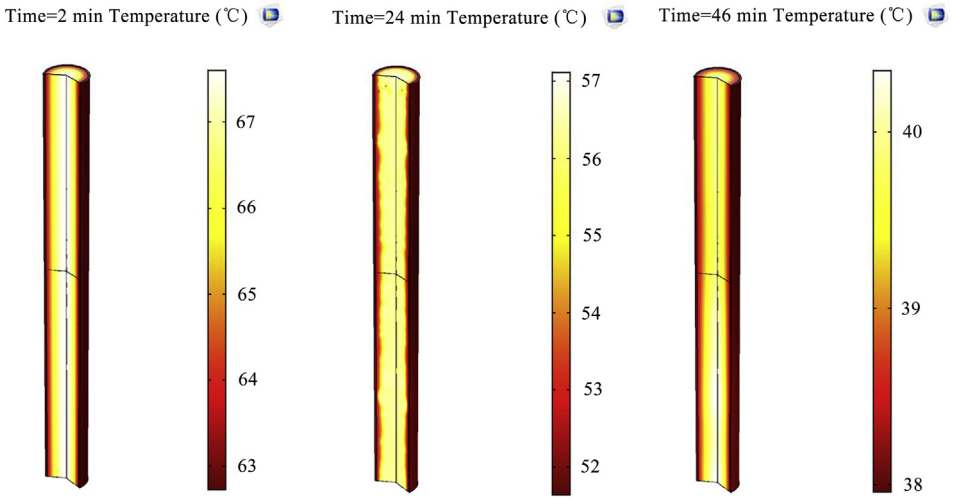

Fig. 7. Temperature distribution of the PCM in the tube with a diameter of 25 mm.

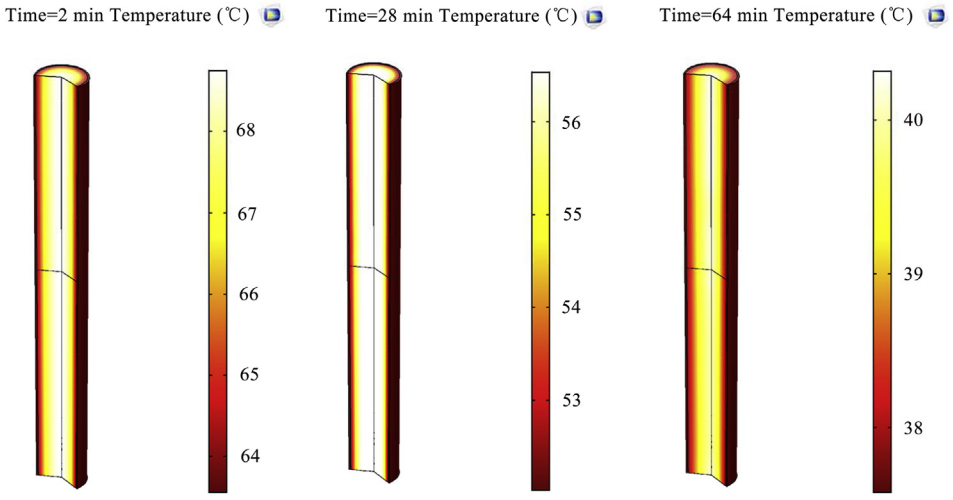

Fig. 8. Temperature distribution of the PCM in the tube with a diameter of 30 mm.

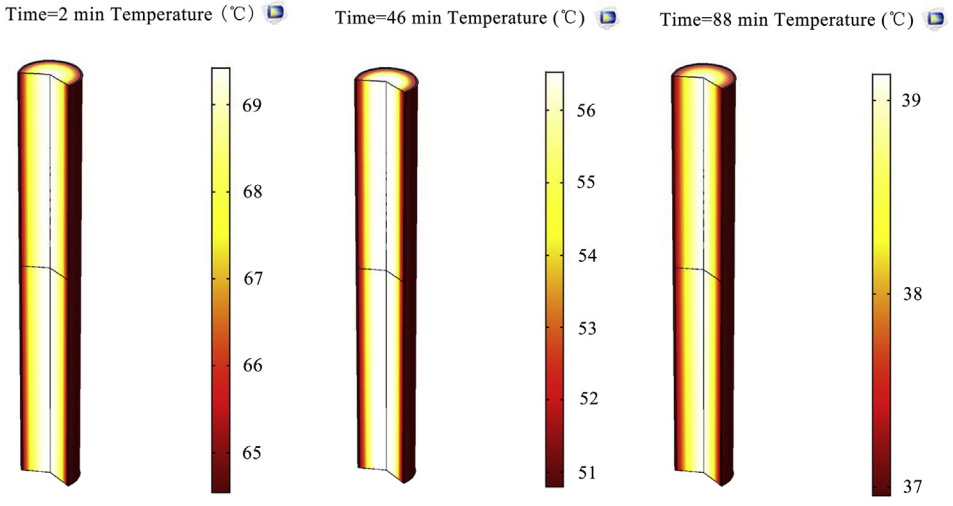

Fig. 9. Temperature distribution of the PCM in the tube with a diameter of 35 mm.

Table 2
Temperature of the PCM in tubes with different diameters at different times.

Location	Next to the tube wall			At the center of the tube		
Diameter	20 mm					
Time (min)	2	14	32	2	14	32
Temperature (°C)	63	54	38	66	56	39
Diameter	25 mm					
Time (min)	2	24	46	2	24	46
Temperature (°C)	63	52	38	67	52	40
Diameter	30 mm					
Time (min)	2	28	64	2	28	64
Temperature (°C)	64	53	38	68	56	40
Diameter	35 mm					
Time (min)	2	46	64	2	46	64
Temperature (°C)	65	51	37	69	56	39

at different times are presented in Table 2.

These findings indicate that, in the tube with a diameter of 20 mm, the temperature of the PCM next to the tube wall was about 63 °C, while that at the center of the tube was 66 °C at 2 min; the difference in temperature between the center and the outer layer was about 3 °C. At 14 min, the temperature of the PCM next to the tube wall was about 54 °C, and that at the center of the tube was 56 °C. During this time, the PCM phase changed, and the difference between the center and the surface was 2 °C. At 32 min, the temperature of the PCM next to the tube wall was about 38 °C, and the temperature at the center of the tube was 39 °C. During this time, all the PCM was solid, and most of the latent heat was released.

In the tube with a 25 mm diameter, the temperature of the PCM next to the tube wall was about 63 °C, and that at the center of the tube was 67 °C at 2 min. At 24 min, the temperature of the PCM next to the tube wall was about 52 °C, and that at the center of the tube was 57 °C; the difference in temperature between the center and the surface was 5 °C. At 46 min, the temperature of the PCM next to the tube wall was about 38 °C, and that at the center of the tube was 40 °C.

In the PCM in tube with a diameter of 30 mm, the temperature of the PCM next to the tube wall was about 64 °C, and that at the center of the tube is 68 °C at 2 min. At 28 min, the temperature of the PCM next to the tube wall was about 53 °C, and that at the center of the tube was 56 °C; the difference between the center and the surface was 3 °C. At 64 min, the temperature of the PCM next to the tube wall was about 38 °C, and that at the center of the tube was 40 °C.

In the PCM in the tube with a 35mm diameter, the temperature of the PCM next to the tube wall was about 65 °C, and that at the center of the tube was 69 °C at 2 min. At 46 min, the temperature of the PCM next to the tube wall was about 51 °C, and that at the center of the tube was 56 °C; the difference between the center and the surface was 5 °C. At 64 min, the temperature of the PCM next to the tube wall was about 37 °C, and that at the center of the tube was 39 °C.

Therefore, for all PCMs under different conditions, the temperature at the surfaces was always the lowest, whereas the temperature at the center of the PCM was the highest. The heat convection on the aluminum tube surfaces was considerably higher than the heat conductivity in the PCM. Thus, the heat on the aluminum surface could be removed by the medium in the drying kiln within a short time, whereas heat transfer from the center of the PCM to the surface area of the PCM tube required an extended period. In addition, the temperature in the PCM decreased over time, and the reduction rates decreased as the diameter of the aluminum tube increased. The reason for this is that heat conduction became extended when the diameter increased.

4.3. Experimental and theoretical temperature at the center of the PCM

Based on the previous findings, the PCM temperature from the center to the surface had the highest temperature and the lowest cooling rate. The central point, namely Point E (as shown in Fig. 3), could be used to determine whether the PCM heat release has been completed. The temperature distribution at the center of the PCM (Point E) from 35 °C to 70 °C is shown in Fig. 10, which indicates that the temperature of the PCM decreased over time, and the reduction rates decreased with the increase in the diameter of the PCM tube. In addition, the temperatures of the PCM in tubes with different diameters were significantly different. Moreover, heat release could be divided into three stages for all the PCMs ranging from 35 °C to 70 °C. The first stage ranged from 70 °C to 57 °C. During this stage, all the PCMs in different tubes had nearly the same temperature over time, with only slight differences in the three situations. The reason for this might be that liquid PCM can shift to different temperature areas, thus enhancing heat transfer in the PCM. Therefore, the effects of the diameter can be ignored, and the PCM in aluminum tubes with different diameters had slightly different temperatures. The second stage ranged from 57 °C to 56 °C for the simulation results, and

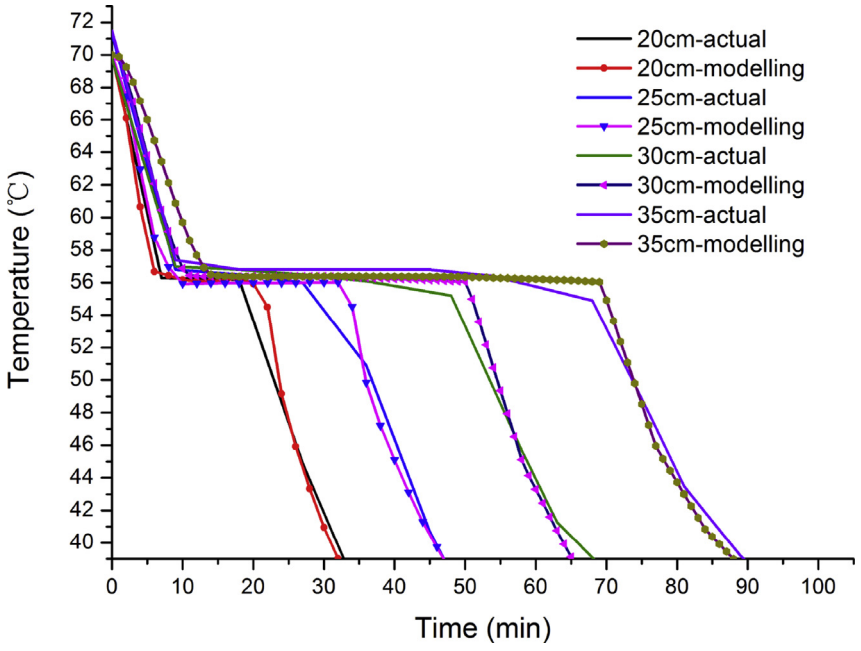

Fig. 10. Central temperature of the PCM in aluminum tubes with different diameters.

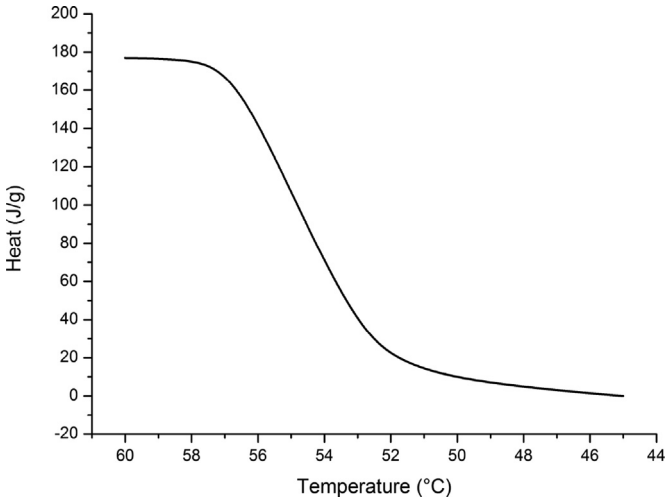

Fig. 11. Ability of the PCM per unit mass to release heat at different temperatures.

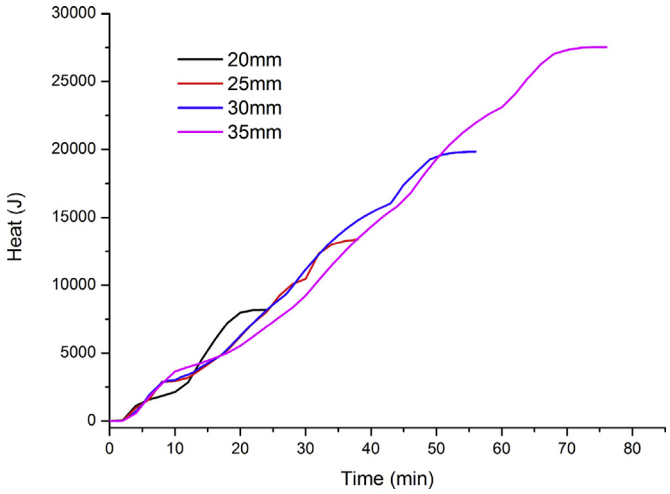

Fig. 13. Total heat release of the PCM in aluminum tubes with different diameters at different times.

from 57 °C to 50 °C for the actual process. During this stage, liquid PCM changed to solid PCM, releasing a large amount of energy; the change in temperature occurred very slowly. The third stage ended at 35 °C. The cooling rates were higher during the third stage than the second stage, but lower than that during the first stage. Most PCMs only decreased in temperature, and no phase change occurred. Thus, only sensible heat release occurred during the first stage, whereas both sensible and latent heat release occurred during the second and third stages. Fig. 10 also shows that the simulation results obtained using Comsol software and the actual processes were similar, except for near the temperature at which phase change occurred. The modeling process had a narrow temperature range for phase change (about 1 °C–2 °C), whereas the actual stage had a relatively wide temperature for phase change (about 2 °C–7 °C). The reason for this is that in the actual process, the temperature of the PCM next to the tube wall decreased after the phase change occurred, whereas in the modeling process, the temperature of the PCM remained the same. Thus, this simulation method could be used to simulate the actual physical process.

4.4. Heat release process

The DSC results indicate that the melting transition of the PCM

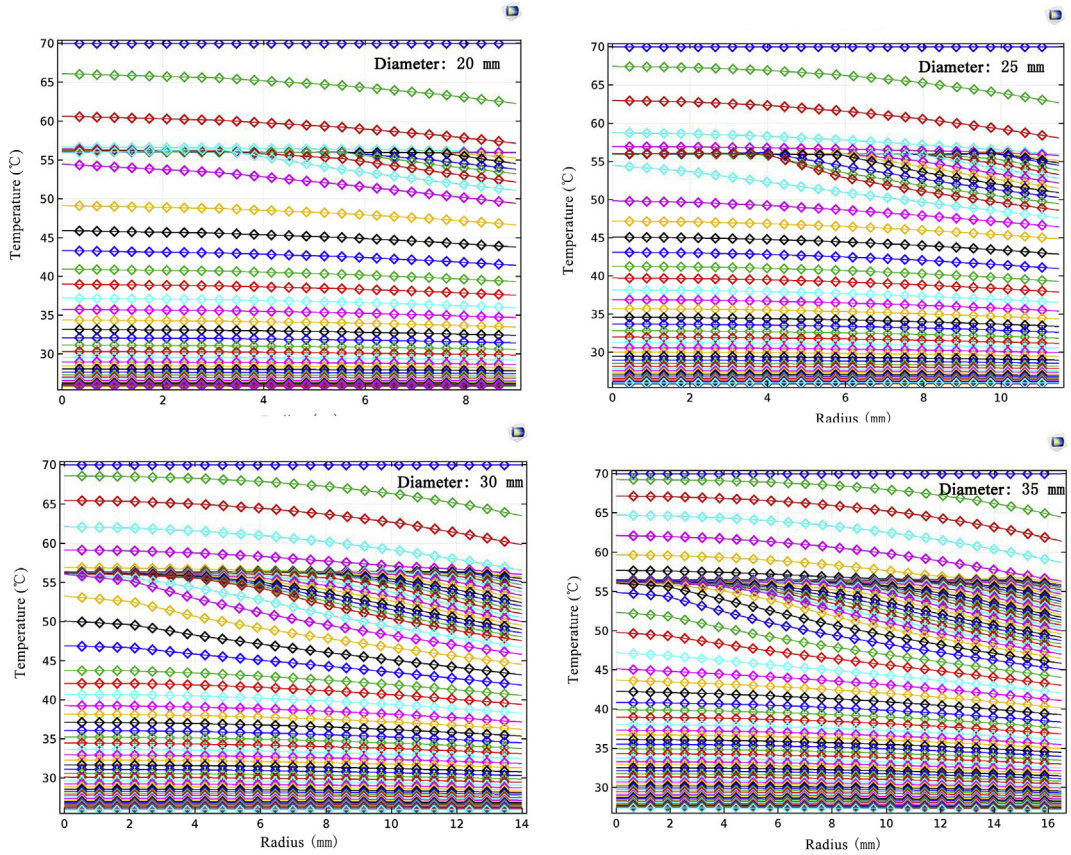

Fig. 12. Temperature distribution in the tubes with different diameters (20, 25, 30 and 35 mm).

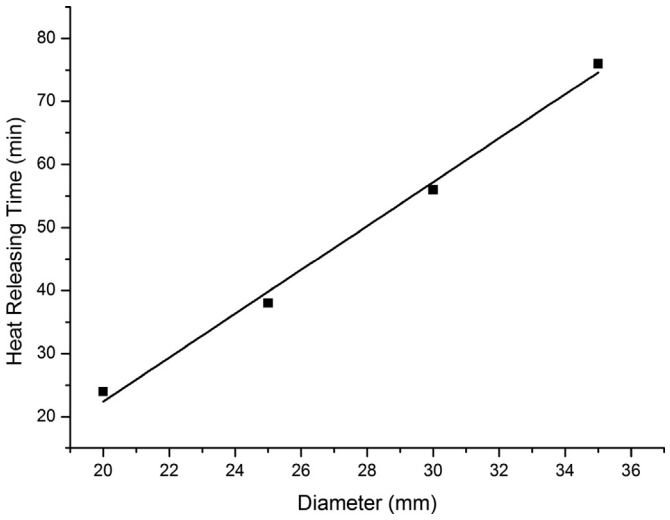

Fig. 14. Relationship between the tube diameter and the time required to complete heat release.

ranged from 45 °C to 60 °C, and the practical application of the PCM in the aluminum tubes demonstrates that most of the heat in the PCM was released at temperatures higher than 45 °C. Moreover, the temperatures of most food, fruit, vegetable, and wood drying exceed 45 °C. Therefore, the heat release of the PCM with temperatures above 45 °C is the most suitable for practical applications.

To evaluate the ability of the PCM to release heat during a phase change, the total amount of energy released per unit mass of the PCM from 45 °C to 60 °C should first be studied. The DSC results, the ability of the PCM to release heat per unit mass from 45 °C to 60 °C, are presented in Fig. 11. The figure indicates that per unit mass, the PCM released about 177 J heat when its temperature varied from 60 °C to 45 °C, 3 J from 60 °C to 57 °C, 164 J from 57 °C to 50 °C, and 10 J from 50 °C to 45 °C; most heat was released from 57 °C to 52 °C. Therefore, the amount of heat released is closely related to the temperature of the PCM.

Based on the aforementioned conclusions that the temperature of the PCM decreased from the center to the surface, the temperature distribution of the PCM at different times and in different areas in the aluminum tube should be determined. Fig. 12 presents the temperature distribution of the PCM at different times in different areas. The aluminum tube had a wall thickness of 1 mm; based on the assumptions, the PCM distribution ranged from 0 mm to 9, 11.5, 14, and 16.5 mm when the aluminum tube had a diameter of 20, 25, 30, and 35mm, respectively. The temperatures were recorded at intervals of 2 min, and each line represents the temperature at different areas in the PCM at the same intervals of 2 min. The temperature decreased from the top of each image to the bottom. Moreover, the coordinate 0 (at the left bottom of the image) represents the center of the PCM.

Fig. 12 shows that the temperatures of the PCM next to the aluminum tube wall were always lower than those at the center of the aluminum tube, and decreased with the increase in radius because heat convection on the aluminum surface drew the energy from the PCM, and this energy was conducted to the aluminum surface for a short time. Moreover, phase change could occur under all conditions during which the temperature is nearly constant. In addition, the heat release process included the release of both latent heat and sensible heat.

To illustrate the heat release process of the PCM in different aluminum tubes, combined with the ability to release heat (shown in Fig. 11), temperature distribution (shown in Fig. 12), and the mass of the PCM in the aluminum tube, the total heat release process is presented in

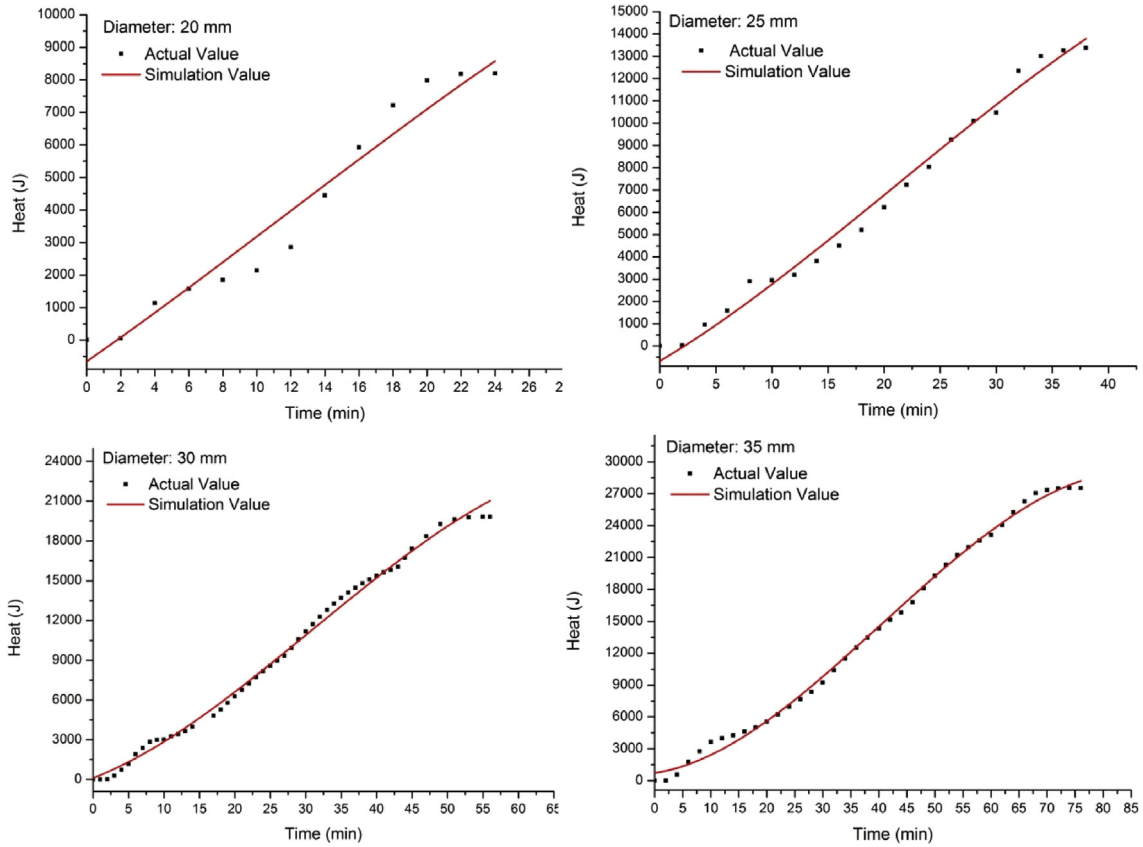

Fig. 15. The actual value and the simulation value of the releasing heat in the tubes with different diameters (20, 25, 30 and 35 mm) at different time based on Eq. (6).

Fig. 13.

Fig. 13 indicates that for the latent energy of the PCM (from 45 °C to 60 °C), the amount of energy increased over time, and the total energy released by the PCM increased linearly with the release time. Moreover, the PCM diameter exerted no significant influence on the energy release rate. The total energy increased with the increase in the diameter of the aluminum tube because the PCM mass increased. Moreover, the PCM in the aluminum tubes with diameters of 20, 25, 30, and 35 mm respectively required 24, 38, 56, and 76 min to complete the heat release process.

To elucidate the effects of the tube diameter on the time required for heat release, the relationship between the tube diameter and time required to complete heat release is presented in Fig. 14. The equation is also given, and R^2 is 0.99 for Eq. (5). Fig. 14 also shows that Eq. (5) can be used to predict the time required for the tubes with different diameters to release heat.

$$\tau = -47.2 + 3.48D \qquad R^2 = 0.997 \tag{5}$$

where τ is the time required for heat release, min; and D is the diameter of the PCM tube, mm.

In addition, the relationship between the amount of heat release and the release time for the PCM in aluminum tubes with different diameters is given by Equation (6), and R^2 is 0.99. The actual value of heat and the value obtained by simulation in accordance with Eq. (6) are shown in Fig. 15. The figure indicates that the value obtained using Eq. (6) is similar to the actual value when the diameter of the PCM tubes ranged from 20 mm to 35 mm and time ranged from 2.5 min to 80 min. Therefore, this equation can be used to predict the heat release process of the PCM in different aluminum tubes.

$$\begin{aligned} Q = 27617.66 &- 3211.09\ D + 292.266\ \tau + 116.62\ D^2 - 6.618\ \tau^2 \\ &+ 16.532\ D\ \tau - 1.338\ D^3 - 0.081\ \tau^3 + 0.471\ D\ \tau^2 \\ &- 0.646\ D^2\tau \qquad R^2 \\ &= 0.99 \end{aligned} \tag{6}$$

5. Conclusions

The melting temperature for PCM ranged from 45 °C to 60 °C, and the latent heat was 177 J/g. The release processes of all PCMs in different aluminum tubes included three stages: two stages of no phase change at temperatures above and lower than the melt transition temperature, respectively, and a phase change stage at a temperature in the melt transition temperature range. The heat release rates were higher during the third stage than the second stage, but lower than that during the first stage. The temperature next to the aluminum tube wall was lower than that at the center of the PCM. Point E at the center of the PCM had the lowest temperature reduction rate, which decreased with the increase in the diameter of the aluminum tube. The PCM temperature obtained by simulation using Comsol software was close to the actual result. The simulation could therefore be applied to actual production. Most of the latent heat was released at temperatures ranging from 57 °C to 50 °C. Only 10 J was released at temperatures ranging from 50 °C to 45 °C, and 3 J was released at temperatures ranging from 60 °C to 57 °C during heat release. The ability of PCM per unit mass to release heat at different temperatures was established based on the DSC results. The total energy released from the PCM increased linearly with the release time, the diameter of the PCM exerted no significant influence on the energy release, and the total energy increased with the increase in the aluminum tube diameter. The PCM in aluminum tubes with diameters of 20, 25, 30, and 35 mm respectively required 24, 38, 56, and 76 min to complete the heat release process. The relationship between the tube diameter and the length of time to complete heat release, and the relationship between the amount of heat released, the diameter of the aluminum tube, and the time to complete the process, were established. These equations can predict the actual value, and can be used to guide practical production.

Declarations

Author contribution statement

Zhengbin He: Conceived and designed the experiments; Wrote the paper.

Songlin Yi: Conceived and designed the experiments; Analyzed and interpreted the data; Contributed reagents, materials, analysis tools or data.

Qian Wan: Performed the experiments; Analyzed and interpreted the data.

Zhenyu Wang: Performed the experiments; Contributed reagents, materials, analysis tools or data.

Jiali Zhang: Analyzed and interpreted the data; Contributed reagents, materials, analysis tools or data.

Funding statement

This work was supported by the Hot Tracking Project in Beijing Forestry University-Wood Solar Synergistic Energy-Saving Drying Technology [2017BLRD04]; the National Key R&D Program of China [2016YFD0600701]; the Fundamental Research Funds for the Central Universities of China [2015ZCQ-CL-01]; and the China Scholarship Council (CSC) scholarship.

Competing interest statement

The authors declare no conflict of interest.

Additional information

No additional information is available for this paper.

References

[1] R. Quadrelli, S. Peterson, The energy–climate challenge: recent trends in CO2 emissions from fuel combustion, Energy Policy 35 (2007) 5938–5952.
[2] L. Bennamoun, Reviewing the experience of solar drying in Algeria with presentation of the different design aspects of solar dryers, Renew. Sustain. Energy Rev. 15 (2011) 3371–3379.
[3] P.J.A.M. Kerkhof, W.J. Coumans, Drying: a fascinating unit operation, Chem. Eng. J. 86 (2002) 1–2.
[4] A. Tiwari, A review on solar drying of agricultural produce, J. Food Process. Technol. 7 (2016) 1–12.
[5] M. Nguyen, W.E. Price, Air-drying of banana: influence of experimental parameters, slab thickness, banana maturity and harvesting season, J. Food Eng. 79 (2007) 200–207.
[6] A. Yataganbaba, İ. Kurtbaş, A scientific approach with bibliometric analysis related to brick and tile drying: a review, Renew. Sustain. Energy Rev. 59 (2016) 206–224.
[7] R. Patil, R. Gawande, A review on solar tunnel greenhouse drying system, Renew. Sustain. Energy Rev. 56 (2016) 196–214.
[8] P. Singh, V. Shrivastava, A. Kumar, Recent developments in greenhouse solar drying: a review, Renew. Sustain. Energy Rev. 82 (2018) 3250–3262.
[9] A.K. Bhardwaj, R. Chauhan, R. Kumar, M. Sethi, A. Rana, Experimental investigation of an indirect solar dryer integrated with phase change material for drying valeriana jatamansi (medicinal herb), Case Stud. Therm. Eng. 10 (2017) 302–314.
[10] A. Agrawal, R.M. Sarviya, Characterization of Commercial Grade Paraffin Wax as Latent Heat Storage Material for Solar Dryers, 2017.
[11] V. Tomar, G.N. Tiwari, B. Norton, Solar dryers for tropical food preservation: thermophysics of crops, systems and components, Sol. Energy 154 (2017) 2–13.
[12] A. Agarwal, R.M. Sarviya, Characterization of commercial grade paraffin wax as latent heat storage material for solar dryers, Mater. Today Proc. 4 (2017) 779–789.
[13] M. Bououd, A. Mechaqrane, Concentration solar dryer water-to-air heat exchanger: modeling and parametric studies, Int. J. Hydrogen Energy 42 (2017) 8631–8643.
[14] S.M. Shalaby, M.A. Bek, A.A. El-Sebaii, Solar dryers with PCM as energy storage medium: a review, Renew. Sustain. Energy Rev. 33 (2014) 110–116.
[15] H. El Hage, A. Herez, M. Ramadan, H. Bazzi, M. Khaled, An investigation on solar drying: a review with economic and environmental assessment, Energy 157 (2018) 815–829.

[16] P.C. Phadke, P.V. Walke, V.M. Kriplani, A review on indirect solar dryers, ARPN J. Eng. Appl. Sci. 10 (2015) 3360–3371.
[17] U. Toshniwal, S. Karale, A review paper on solar dryer, Int. J. Eng. Res. Afr. 3 (2013) 896–902.
[18] H. Lund, Renewable energy strategies for sustainable development, Energy 32 (2007) 912–919.
[19] Y. Wang, X. Yang, T. Xiong, W. Li, K.W. Shah, Performance evaluation approach for solar heat storage systems using phase change material, Energy Build. 155 (2017) 115–127.
[20] Z. Zhou, J. Liu, C. Wang, X. Huang, F. Gao, S. Zhang, B. Yu, Research on the application of phase-change heat storage in centralized solar hot water system, J. Clean. Prod. 198 (2018) 1262–1275.
[21] S. Thaker, A. Olufemi Oni, A. Kumar, Techno-economic evaluation of solar-based thermal energy storage systems, Energy Convers. Manag. 153 (2017) 423–434.
[22] M. Seitz, M. Johnson, S. Hübner, Economic impact of latent heat thermal energy storage systems within direct steam generating solar thermal power plants with parabolic troughs, Energy Convers. Manag. 143 (2017) 286–294.
[23] M. Faegh, M.B. Shafii, Experimental investigation of a solar still equipped with an external heat storage system using phase change materials and heat pipes, Desalination 409 (2017) 128–135.
[24] X. Feng, Design and Performance Research of a Solar wood Dryer with Latent Heat Storage System, Beijing Forestry University, 2010.
[25] A.K. Babu, G. Kumaresan, V.A.A. Raj, R. Velraj, Review of leaf drying: mechanism and influencing parameters, drying methods, nutrient preservation, and mathematical models, Renew. Sustain. Energy Rev. 90 (2018) 536–556.
[26] N. Sarier, E. Onder, Organic Phase Change Materials and Their Application: an Overview, 2012.
[27] A. Sarı, A. Karaipekli, Thermal conductivity and latent heat thermal energy storage characteristics of paraffin/expanded graphite composite as phase change material, Appl. Therm. Eng. 27 (2007) 1271–1277.
[28] N. Ukrainczyk, S. Kurajica, J. Šipušić, Thermophysical comparison of five commercial paraffin waxes as latent heat storage materials, Chem. Biochem. Eng. Q. 24 (2010) 129–137.
[29] A.S. Fleischer, Thermal Energy Storage Using Phase Change Materials: Fundamentals and Applications, Springer, 2015.